

# Heat capacity of square-well fluids of variable width

J. Largo\* and J. R. Solana†

*Departamento de Física Aplicada, Universidad de Cantabria, 39005 Santander, Spain*

L. Acedo‡ and A. Santos§

*Departamento de Física, Universidad de Extremadura, 06071 Badajoz, Spain*

(Dated: May 22, 2019)

We have obtained by Monte Carlo NVT simulations the constant-volume excess heat capacity of square-well fluids for several temperatures, densities and potential widths. Heat capacity is a thermodynamic property much more sensitive to the accuracy of a theory than other thermodynamic quantities, such as the compressibility factor. This is illustrated by comparing the reported simulation data for the heat capacity with the theoretical predictions given by the Barker–Henderson perturbation theory as well as with those given by a non-perturbative theoretical model based on Baxter’s solution of the Percus–Yevick integral equation for sticky hard spheres. Both theories give accurate predictions for the equation of state. By contrast, it is found that the Barker–Henderson theory strongly underestimates the excess heat capacity for low to moderate temperatures, whereas a much better agreement between theory and simulation is achieved with the non-perturbative theoretical model, although the accuracy of the latter worsens for high densities and low temperatures, especially for large well widths.

## I. INTRODUCTION

Thermodynamic and structural properties of square-well (SW) fluids have been profusely studied both from theory and from computer simulation [1]–[38]. From the theoretical side, the first few virial coefficients have been obtained [1, 2, 37] and the radial distribution function has been evaluated from numerical solutions of integral equation theories, such as Percus–Yevick [6, 7, 8, 30, 38], Yvon–Born–Green [14], HNC [10], MSA [16, 30], Rogers–Young [28], ORPA [28], and HRT [35]. Simpler analytical approximations have also been proposed [11, 12, 19, 20, 21, 22, 34]. The thermodynamic properties have been derived from the theoretical structure functions as well as from perturbation theory [3, 4, 9, 13, 23, 27]. Access to the “experimental” properties of SW fluids has been made possible via molecular dynamics and Monte Carlo simulations [5, 10, 13, 16, 17, 18, 26, 36, 38]. Special attention has received the determination of the critical point of SW fluids [6, 7, 8, 13, 18, 23, 25, 26, 29, 33, 34, 35, 38], both from the theoretical and simulational viewpoints. The main reason for this wide interest lies in the fact that a SW fluid is perhaps the simplest one whose particles have attractive as well as repulsive interactions. In general, theories are easier to apply to SW fluids than to other fluids with more realistic potentials. In addition, the SW potential seems to be particularly sensitive to the performance of a theory. Therefore, this kind of fluid is an excellent testing-ground for many theories of fluids and so the study of SW fluids can be considered as a first step towards our understanding of the properties of fluids with more sophisticated interactions. There is an additional reason explaining the recent revival of interest in SW fluids. The SW potential possesses, besides the diameter of the hard core and the depth of the well, an additional parameter measuring the width of the well. This makes the SW potential with a small width especially suited to model the effective interactions among colloidal particles [16, 28, 30, 31, 38]. In this context, the glass transition [30, 31] and a solid-to-solid isostructural transition [24] have been studied for narrow SW systems.

Despite the extensive number of studies devoted to the SW fluid, relatively little attention has been paid to several thermodynamic properties. This is the case for the heat capacity. To the best of our knowledge, there are available [5, 10] only a few simulation data of this property for SW fluids. Theoretical calculations of the same quantity are equally scarce [10]. In the present paper we have carried out Monte Carlo simulations of the constant-volume excess heat capacity  $C_V^E$  of SW fluids for several values of the potential width and, for each of them, for several densities and temperatures. Moreover, in order to put clear the sensitivity of this property to the accuracy of a theory, the simulation data are compared with the results obtained from the Barker–Henderson (BH) [39, 40] perturbation theory

---

\*Electronic address: largoju@unican.es

†Electronic address: solana jr@unican.es; Author to whom correspondence should be addressed

‡Electronic address: acedo@unex.es

§Electronic address: andres@unex.es

and with those derived from the theoretical model proposed by Yuste and Santos [22], recently simplified by Acedo and Santos [34].

The paper is organized as follows. In the next section, we summarize the theoretical foundations of the MC procedure used and we describe the simulations performed and the results obtained. In Section III, we present an outline of the above-mentioned theories. Finally, in the last section the theoretical results are compared with simulation data and discussed.

## II. MONTE CARLO SIMULATIONS

In a square-well (SW) fluid, particles interact by means of a potential of the form

$$u(r) = \begin{cases} \infty & \text{if } r \leq \sigma \\ -\epsilon & \text{if } \sigma < r \leq \lambda\sigma \\ 0 & \text{if } r > \lambda\sigma \end{cases} \quad (1)$$

where  $\lambda$  is the potential width in units of the particle diameter  $\sigma$  and  $\epsilon$  is the potential depth.

Constant-volume averaged excess heat capacity per particle in a SW fluid can be expressed in the form [5]:

$$\frac{C_V^E}{Nk} = \frac{1}{T^{*2}} \frac{\langle (M - \langle M \rangle)^2 \rangle}{N}, \quad (2)$$

where  $N$  is the number of particles,  $k$  is the Boltzmann constant,  $T^* = kT/\epsilon$  is the reduced temperature, and  $M$  is the number of pairs of interacting particles, that is, the number of pairs of particles whose centers lie separated by a reduced distance  $r^* = r/\sigma \leq \lambda$ .

The averages involved in equation (2) can be calculated by Monte Carlo (MC) simulations in the NVT ensemble. Therefore, we have proceeded to calculate by means of MC NVT the constant-volume averaged excess heat capacity per particle for SW fluids with well widths  $\lambda$  ranging from 1.1 to 1.5. For each value of  $\lambda$ ,  $C_V^E$  has been evaluated for several densities along isotherms. To this end, a system consisting of 512 particles placed in a cubic box with periodic boundary conditions was used. Particles were initially placed in a regular configuration and then the system was allowed to equilibrate for  $2 \times 10^4$  cycles, each of them consisting of an attempt move per particle, the first  $10^4$  cycles at a very high temperature and the remaining ones at the desired temperature. The calculation of  $C_V^E$  was performed by averaging over the next  $5 \times 10^5$  cycles, performing partial averages every  $10^4$  cycles with the aim of estimating the statistical error from the standard deviation. The use of such a huge number of cycles in the calculations was motivated by the need of ensuring that the values of  $C_V^E$  converged to a constant value, apart from statistical fluctuations. In fact, we realized that for low values of the number of cycles used in the calculations, the values of  $C_V^E$  increase with the number of cycles used.

The results are shown in Table I. We have considered four isotherms for  $\lambda = 1.1, 1.2, 1.3$  and three isotherms for  $\lambda = 1.5$ . The lowest temperature in each case is larger than the estimated critical temperature [13, 18, 23, 25, 26, 33, 34, 35]:  $T_c^* \simeq 0.5, 0.6, 0.8, 1.2$  for  $\lambda = 1.1, 1.2, 1.3, 1.5$ , respectively.

## III. THEORY

### A. Barker–Henderson perturbation theory

In the second-order Barker–Henderson perturbation theory [39, 40], the free energy is expressed in the form

$$\frac{F}{NkT} = \frac{F_0}{NkT} + \frac{F_1}{NkT} \frac{1}{T^*} + \frac{F_2}{NkT} \frac{1}{T^{*2}}, \quad (3)$$

where  $F_0$  is the free energy of the hard-sphere (HS) reference system and  $F_1$  and  $F_2$  are the first- and second-order perturbative terms, respectively. According to this theory, the constant-volume excess heat capacity per particle is given by

$$\frac{C_V^E}{Nk} = -\frac{2}{T^{*2}} \frac{F_2}{NkT}, \quad (4)$$

where

$$\frac{F_2}{NkT} = -\pi\rho kT \left( \frac{\partial\rho}{\partial P} \right)_0 \int_0^\infty [u_1^*(r)]^2 g_0(r) r^2 dr \quad (5)$$

in the so-called *macroscopic compressibility approximation*, whereas

$$\frac{F_2}{NkT} = -\pi\rho kT \int_0^\infty [u_1^*(r)]^2 \left\{ \frac{\partial [\rho g_0(r)]}{\partial P} \right\}_0 r^2 dr \quad (6)$$

in the so-called *local compressibility approximation*. In Eqs. (5) and (6),  $\rho = N/V$  is the number density,  $u_1^*(r) = u_1(r)/\epsilon$  is the perturbative contribution to the potential function, which in a SW potential is  $u_1^*(r) = -1$  for  $\sigma < r < \lambda\sigma$ ,  $P$  is the pressure, and  $g_0(r)$  is the radial distribution function (r.d.f.) of the hard-sphere reference fluid.

In recent years, several analytical and very accurate expressions for the r.d.f.  $g_0(r)$  of the HS fluid have been proposed [41, 42, 43]. They can be used to determine  $F_2$  in expressions (5) and (6). Regarding  $(\partial\rho/\partial P)_0$ , which appears explicitly in expression (5) and implicitly in (6), it can be obtained from the well-known Carnahan–Starling [44] equation of state

$$Z_0 = \frac{P_0 V}{NkT} = \frac{1 + \eta + \eta^2 - \eta^3}{(1 - \eta)^3}, \quad (7)$$

where  $\eta = (\pi/6)\rho\sigma^3$  is the packing fraction.

### B. Yuste–Acedo–Santos model

The internal energy can be obtained from the r.d.f  $g(r)$  through the energy equation

$$U = \frac{3}{2}NkT + 2\pi N\rho \int_0^\infty u(r) g(r) r^2 dr, \quad (8)$$

whence

$$\frac{C_V^E}{Nk} = \frac{2\pi\rho}{k} \int_0^\infty u(r) \left[ \frac{\partial g(r)}{\partial T} \right]_V r^2 dr. \quad (9)$$

In the special case of the SW potential (1), Eqs. (8) and (9) become

$$U = \frac{3}{2}NkT - 12N\epsilon\eta \int_1^\lambda g(r^*) r^{*2} dr^*, \quad (10)$$

$$\frac{C_V^E}{Nk} = -12\eta \int_1^\lambda \left[ \frac{\partial g(r^*)}{\partial T^*} \right]_\eta r^{*2} dr^*, \quad (11)$$

respectively. The r.d.f  $g(r^*)$  of the SW fluid depends on the packing fraction  $\eta$ , the reduced temperature  $T^*$  and, parametrically, on the well width  $\lambda$ . In principle, one has to resort to numerical solutions of integral equation theories. On the other hand, particularly suitable for the purpose of obtaining the heat capacity is the heuristic model proposed by Yuste and Santos [22] and recently simplified by Acedo and Santos [34], which is analytical and fairly accurate.

Henceforth we will refer to this model as the Yuste–Acedo–Santos (YAS) model. It is based on expressing the Laplace transform  $G(t)$  of  $r^*g(r^*)$  in the form

$$G(t) = t \frac{F(t) e^{-t}}{1 + 12\eta F(t) e^{-t}} = \sum_{n=1}^{\infty} (-12\eta)^{n-1} t [F(t)]^n e^{-nt}, \quad (12)$$

where the auxiliary function  $F(t)$  is assumed to have the form [22, 34]

$$F(t) = -\frac{1}{12\eta} \frac{e^{1/T^*} + K_1 t - (e^{1/T^*} - 1 + K_2 t) e^{-(\lambda-1)t}}{1 + S_1 t + S_2 t^2 + S_3 t^3}. \quad (13)$$

The coefficients  $K_1$ ,  $K_2$ ,  $S_1$ ,  $S_2$  and  $S_3$  are *explicit* functions of  $\eta$ ,  $T^*$  and  $\lambda$  determined from consistency conditions. We refer the interested reader to Refs. [22, 34] for further details. The YAS model (13) reduces to the exact solutions of the Percus–Yevick (PY) equation in the limit of hard spheres ( $\lambda \rightarrow 1$  or  $T^* \rightarrow \infty$ ) [45, 46], as well as in the limit of sticky hard spheres ( $\lambda \rightarrow 1$  and  $T^* \rightarrow 0$  with  $T^* \sim -1/\ln(\lambda-1)$ ) [47]. From that point of view, the approximation (13) can be seen as a simple extension to finite widths of Baxter’s solution of the PY equation for sticky hard spheres.

Upon Laplace inversion of Eq. (12), the final expression of the r.d.f. reads

$$g(r^*) = r^{*-1} \sum_{n=1}^{\infty} (-12\eta)^{n-1} f_n(r^* - n) \Theta(r^* - n), \quad (14)$$

where the functions  $f_n(r^*)$  are the inverse Laplace transforms of  $t[F(t)]^n$  and  $\Theta(r^*)$  is Heaviside’s step function. Therefore, to determine the r.d.f. for  $r^* < n+1$  only the first  $n$  terms in the summation (14) are needed. In particular, for the values of  $\lambda \leq 2$  considered in this paper, one has

$$g(r^*) = -\frac{r^{*-1}}{12\eta} \sum_{i=1}^3 z_i \frac{e^{1/T^*} + K_1 z_i}{S_1 + 2S_2 z_i + 3S_3 z_i^2} e^{z_i(r^*-1)}, \quad 1 < r^* \leq \lambda, \quad (15)$$

where  $z_i$  ( $i = 1, 2, 3$ ) are the three roots of the cubic equation  $1 + S_1 t + S_2 t^2 + S_3 t^3 = 0$ . Inserting Eq. (15) into Eq. (11), we finally get

$$\frac{C_V^E}{Nk} = \frac{\partial}{\partial T^*} \sum_{i=1}^3 \frac{e^{1/T^*} + K_1 z_i}{S_1 + 2S_2 z_i + 3S_3 z_i^2} \left[ z_i^{-1} - 1 + (\lambda - z_i^{-1}) e^{z_i(\lambda-1)} \right]. \quad (16)$$

The heat capacity can also be obtained from the YAS r.d.f. by following the virial and compressibility routes to the equation of state. The reason for the choice of the energy route (8) is two-fold. First, it is obviously the most direct route to determine the heat capacity. Second, we have checked that the other routes yield results that present larger deviations from the simulation data. This latter observation is consistent with the case of the PY theory for sticky hard spheres [48] and for SW fluids [7, 8].

#### IV. RESULTS AND DISCUSSION

Results obtained for  $C_V^E$  from the Barker–Henderson perturbation theory within the local compressibility approximation as well as within the macroscopic compressibility equation are compared in Figs. 1–4 with the simulation data of Table I. We can see that although the local compressibility approximation provides a better agreement with simulation data, both approximations are rather poor at low temperatures, in contrast with the situation for the equation of state [39, 49], which is accurately given by the BH perturbation theory even at relatively low temperatures for wide ranges of densities and potential wells. The reason is that, as pointed before, the constant-volume excess heat capacity is a thermodynamic property particularly sensitive to the performance of a theory and therefore the influence of higher order terms, which is small in the equation of state, may be important in the heat capacity. This is particularly true for low values of the potential width, since the lower the potential width, the slower the convergence of the BH perturbation theory at low temperatures [15].

A much better agreement is obtained with YAS theory, Eq. (16), as shown in the same figures. This theory, in contrast to the BH theory, provides a better agreement with the simulation data of  $C_V^E$  as the potential width decreases. This is consistent with the fact that, as said before, the YAS model is an extension to  $\lambda > 1$  of the PY

solution for sticky hard spheres and hence it is expected to be as accurate as the PY theory at least for small  $\lambda - 1$ . The structural properties predicted by the YAS model for the SW fluid also exhibits a good agreement with simulation data for low values of  $\lambda - 1$  whereas the accuracy worsens as  $\lambda$  increases [22, 34]. Figures 1–4 show that, given a well width  $\lambda$ , the YAS values of  $C_V^E$  are more accurate as the temperature increases and/or the density decreases.

In conclusion, we have performed Monte Carlo simulations of the constant-volume excess heat capacity of SW fluids of variable width for a wide range of densities and at several characteristic temperatures. This thermodynamic quantity vanishes for hard spheres and so it represents an important measure of the influence of attractive forces on the state of the fluid. Moreover, the heat capacity seems to provide a rather stringent test to assess the accuracy of theoretical approaches. In this paper we have compared the simulation data with the Barker–Henderson perturbation theory [39, 40] and with a non-perturbative theory developed by Yuste, Acedo, and Santos [22, 34]. While the former theory presents a poor performance, the non-perturbative theory does a fairly good job, especially for narrow wells, except at low temperatures and high densities. Therefore, as several theories for SW fluids have achieved a considerable accuracy for the equation of state and the pair correlation function of SW fluids, the constant volume excess heat capacity seems to be a suitable thermodynamic property to discriminate between them. In this context, we expect that our simulation data can stimulate other studies on the heat capacity of SW fluids of variable width and can be used to check the reliability of other approximations.

The present work has been partially supported by the Spanish Dirección General de Investigación (DGI) under grants No. BFM2000-0014 (J.L. and J.R.S) and No. BFM2001-0718 (L.A and A.S.).

- 
- [1] KATSURA, S., 1959, *Phys. Rev.* **115**, 1417.
  - [2] BARKER, J. A., AND HENDERSON D., 1967, *Can. J. Phys.* **44**, 3959.
  - [3] SMITH, W. R., HENDERSON, D., AND BARKER, J. A., 1970, *J. Chem. Phys.* **53**, 508.
  - [4] SMITH, W. R., HENDERSON, D., AND BARKER, J. A., 1971, *J. Chem. Phys.* **55**, 4027.
  - [5] ALDER, B. J., YOUNG, D. A., AND MARK, M. A., 1972, *J. Chem. Phys.* **56**, 3013.
  - [6] TAGO, Y., 1973, *J. Chem. Phys.* **58**, 2096.
  - [7] TAGO, Y., 1973, *Phys. Lett. A* **44**, 43.
  - [8] TAGO, Y., 1974, *J. Chem. Phys.* **60**, 1528.
  - [9] HENDERSON, D., BARKER, J. A., AND SMITH, W. R., 1976, *J. Chem. Phys.* **64**, 4244.
  - [10] HENDERSON, D., MADDEN, W. G., AND FITTS, D. D., 1976, *J. Chem. Phys.* **64**, 5026.
  - [11] NEZBEDA, I., 1977, *Czech. J. Phys. B* **27**, 247.
  - [12] SHARMA, R. V., AND SHARMA, K. C., 1977, *Physica A* **89**, 213.
  - [13] HENDERSON, D., SCALISE, O. H., AND SMITH, W. R., 1980, *J. Chem. Phys.* **72**, 2431.
  - [14] JONES, G. L., KOZAK, J. J., LEE, E., FISHMAN, S., AND FISHER, M. E., 1981, *Phys. Rev. Lett.* **46**, 795.
  - [15] HENDERSON, D., 1983, *J. Chem. Phys.* **79**, 6430.
  - [16] HUANG, J. S., SAFRAN, S. A., KIM, M. W., AND GREEST, G. S., 1984, *Phys. Rev. Lett.* **53**, 592.
  - [17] DE LONNGI, D. A., LONGGI, P. A., AND ALEJANDRE, J., 1990, *Mol. Phys.* **71**, 427.
  - [18] VEGA, L., DE MIGUEL, E., RULL, L. F., JACKSON, G., AND MCLURE, I. A., 1992, *J. Chem. Phys.* **96**, 2296.
  - [19] TANG, Y., AND LU, B. C.-Y., 1993, *J. Chem. Phys.* **99**, 9828.
  - [20] TANG, Y., AND LU, B. C.-Y., 1994, *J. Chem. Phys.* **100**, 3079.
  - [21] TANG, Y., AND LU, B. C.-Y., 1994, *J. Chem. Phys.* **100**, 6665.
  - [22] YUSTE, S. B., AND SANTOS, A., 1994, *J. Chem. Phys.* **101**, 2355.
  - [23] CHANG, J., AND SANDLER, S. I., 1994, *Mol. Phys.* **81**, 745.
  - [24] LIKOS, C. N., AND SENATORE, G., 1995, *J. Phys.: Condens. Matter* **7**, 6797.
  - [25] BRILLIANTOV, N. V., AND VALLEAU, J. P., 1998, *J. Chem. Phys.* **108**, 1123.
  - [26] ELLIOTT, J. R., AND HU, L., 1999, *J. Chem. Phys.* **110**, 3043.
  - [27] BENAVIDES, A. L., AND GIL-VILLEGAS, A., 1999, *Mol. Phys.* **97**, 1225.
  - [28] LANG, A., KAHL, G., LIKOS, C. N., LÖWEN, H., AND WATZLAWEK, M., 1999, *J. Phys.: Condens. Matter* **11**, 10143.
  - [29] NORO, M. G., AND FRENKEL, D., 2000, *J. Chem. Phys.* **113**, 2941.
  - [30] DAWSON, K., FOFFI, G., FUCHS, M., GÖTZE, W., SCIORTINO, F., SPERL, M., TARTAGLIA, P., VOIGTMANN, TH., AND ZACCARELLI, E., 2001, *Phys. Rev. E* **63**, 011401.
  - [31] ZACCARELLI, E., FOFFI, G., DAWSON, K. A., SCIORTINO, F., AND TARTAGLIA, P., 2001, *Phys. Rev. E* **63**, 031501.
  - [32] ACEDO, L., 2000, *J. Stat. Phys.* **99**, 707.
  - [33] VLIEGENTHART, G. A., AND LEKKERKERKER, H. N. W., 2000, *J. Chem. Phys.* **112**, 5364.
  - [34] ACEDO, L., AND SANTOS, A., 2001, *J. Chem. Phys.* **115**, 2805.
  - [35] REINER, A., AND KAHL, G., 2002, *J. Chem. Phys.* **117**, 4925.
  - [36] LARGO, J., AND SOLANA, J. R., 2002, *Fluid Phase Equilib.* **193**, 277.

- [37] VLASOV, A. Y., YOU, X.-M., AND MASTERS, A. J., 2002, *Mol. Phys.* **100**, 3313.
- [38] ZACCARELLI, E., FOFFI, G., DAWSON, K. A., BULDYREV, S. V., SCIORTINO, F., AND TARTAGLIA, P., 2003, *J. Phys.: Condens. Matter* **15**, S367.
- [39] BARKER, J. A., AND HENDERSON, D., 1967, *J. Chem. Phys.* **47**, 2856.
- [40] BARKER, J. A., AND HENDERSON, D., 1967, *J. Chem. Phys.* **47**, 4714.
- [41] YUSTE, S. B., AND SANTOS, A., 1991, *Phys. Rev. A* **43**, 5418.
- [42] YUSTE, S. B., LÓPEZ DE HARO, M., AND SANTOS, A., 1996, *Phys. Rev. E* **53**, 4820.
- [43] TANG, Y., AND LU, B. C.-Y., 1995, *J. Chem. Phys.* **103**, 7463.
- [44] CARNAHAN, N. F., AND STARLING, K. E., 1969, *J. Chem. Phys.* **51**, 635.
- [45] WERTHEIM, M. S., 1963, *Phys. Rev. Lett.* **10**, 321.
- [46] THIELE, E., 1963, *J. Chem. Phys.* **39**, 474.
- [47] BAXTER, R. J., 1968, *J. Chem. Phys.* **49**, 2770.
- [48] WATS, R. O., HENDERSON, D., AND BAXTER, R. J., 1971, *Adv. Chem. Phys.* **21**, 421.
- [49] LARGO, J., AND SOLANA, J. R., unpublished work.

TABLE I: MC simulation data for  $C_V^E/Nk$ . The numbers enclosed between parentheses indicate the statistical uncertainty in the last decimal places.

| $\rho^*$        | $T^* = 0.7$ | $T^* = 1.0$ | $T^* = 1.5$ | $T^* = 2.0$ | $T^* = 2.5$ |
|-----------------|-------------|-------------|-------------|-------------|-------------|
| $\lambda = 1.1$ |             |             |             |             |             |
| 0.1             | 0.527(3)    | 0.1731(8)   | 0.0580(2)   |             |             |
| 0.2             | 0.94(1)     | 0.319(1)    | 0.1109(3)   | 0.0556(2)   |             |
| 0.3             | 1.25(2)     | 0.431(3)    | 0.1588(8)   |             |             |
| 0.4             | 1.40(2)     | 0.525(5)    | 0.1979(9)   | 0.1033(4)   |             |
| 0.5             | 1.51(3)     | 0.603(7)    | 0.230(1)    |             |             |
| 0.6             | 1.50(3)     | 0.630(7)    | 0.252(2)    | 0.1361(7)   |             |
| 0.7             | 1.42(3)     | 0.612(7)    | 0.261(3)    |             |             |
| 0.8             | 1.38(2)     | 0.595(6)    | 0.256(3)    | 0.142(1)    |             |
| 0.9             | 1.15(3)     | 0.534(7)    | 0.241(4)    |             |             |
| $\lambda = 1.2$ |             |             |             |             |             |
| 0.1             |             | 0.367(2)    | 0.1155(3)   | 0.0559(1)   |             |
| 0.2             | 3.11(17)    | 0.621(7)    | 0.1988(6)   | 0.0979(3)   |             |
| 0.3             |             | 0.77(1)     | 0.2568(9)   | 0.1288(6)   |             |
| 0.4             | 3.68(22)    | 0.83(1)     | 0.282(2)    | 0.1463(6)   |             |
| 0.5             |             | 0.82(1)     | 0.295(2)    | 0.1528(6)   |             |
| 0.6             | 3.01(14)    | 0.743(9)    | 0.282(3)    | 0.1459(8)   |             |
| 0.7             |             | 0.657(8)    | 0.253(2)    | 0.1351(7)   |             |
| 0.8             | 1.35(5)     | 0.530(8)    | 0.222(2)    | 0.1209(9)   |             |
| 0.9             |             | 0.463(6)    | 0.195(2)    | 0.111(1)    |             |
| $\lambda = 1.3$ |             |             |             |             |             |
| 0.1             |             |             | 0.1846(6)   | 0.0864(2)   | 0.0504(1)   |
| 0.2             |             | 1.17(1)     | 0.303(2)    | 0.1423(7)   | 0.0834(3)   |
| 0.3             |             |             | 0.359(4)    | 0.1720(5)   | 0.1016(4)   |
| 0.4             |             | 1.35(2)     | 0.363(2)    | 0.178(1)    | 0.1060(6)   |
| 0.5             |             |             | 0.340(3)    | 0.1688(8)   | 0.1019(7)   |
| 0.6             |             | 0.90(2)     | 0.289(3)    | 0.151(1)    | 0.0918(3)   |
| 0.7             |             |             | 0.251(2)    | 0.1350(9)   | 0.0838(5)   |
| 0.8             |             | 0.512(8)    | 0.226(2)    | 0.126(1)    | 0.0807(6)   |
| 0.9             |             |             | 0.219(2)    | 0.122(1)    | 0.078(1)    |
| $\lambda = 1.5$ |             |             |             |             |             |
| 0.1             |             |             | 0.426(3)    | 0.1724(4)   | 0.0952(3)   |
| 0.2             |             |             | 0.705(5)    | 0.263(2)    | 0.1426(8)   |
| 0.3             |             |             | 0.719(9)    | 0.277(2)    | 0.1495(7)   |
| 0.4             |             |             | 0.563(5)    | 0.239(2)    | 0.1339(8)   |
| 0.5             |             |             | 0.401(6)    | 0.190(2)    | 0.1142(6)   |
| 0.6             |             |             | 0.295(2)    | 0.161(1)    | 0.1027(5)   |
| 0.7             |             |             | 0.270(2)    | 0.1513(6)   | 0.0977(6)   |
| 0.8             |             |             | 0.235(3)    | 0.136(1)    | 0.0894(9)   |
| 0.9             |             |             | 0.188(2)    | 0.109(2)    | 0.0716(6)   |

## List of figures

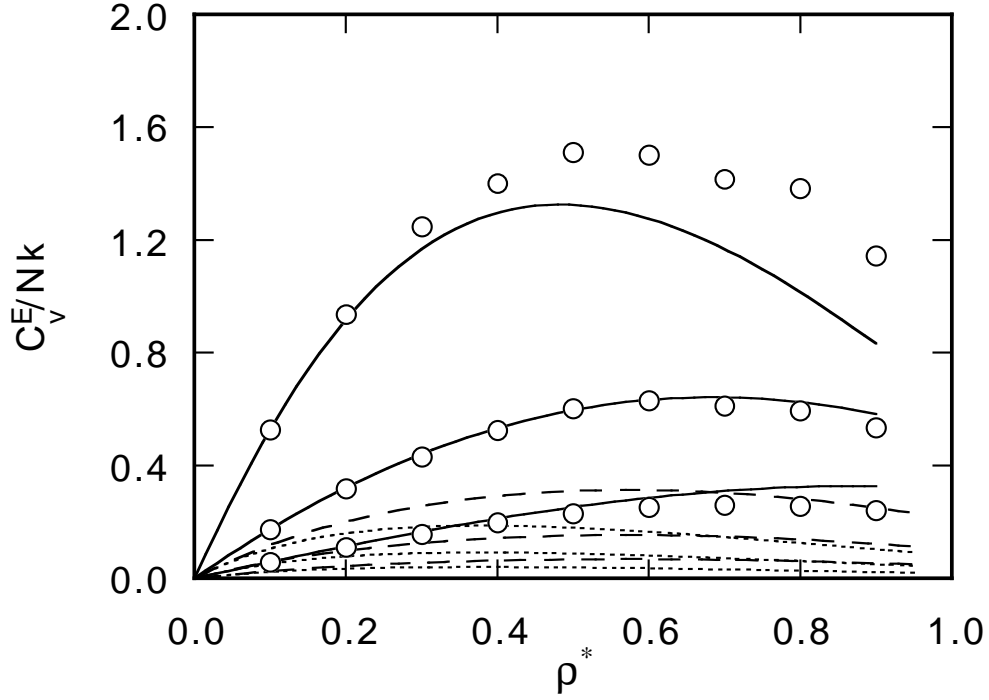


FIG. 1: Constant-volume excess heat capacity for a SW fluid with  $\lambda = 1.1$  as a function of the reduced density  $\rho^*$ . Circles: simulation data from Table I for  $T^* = 0.7$ ,  $T^* = 1.0$ , and  $T^* = 1.5$ , respectively, from top to down. Continuous curve: YAS model. Dashed curve: BH perturbation theory in the local compressibility approximation. Dotted curve: BH perturbation theory in the macroscopic compressibility approximation.



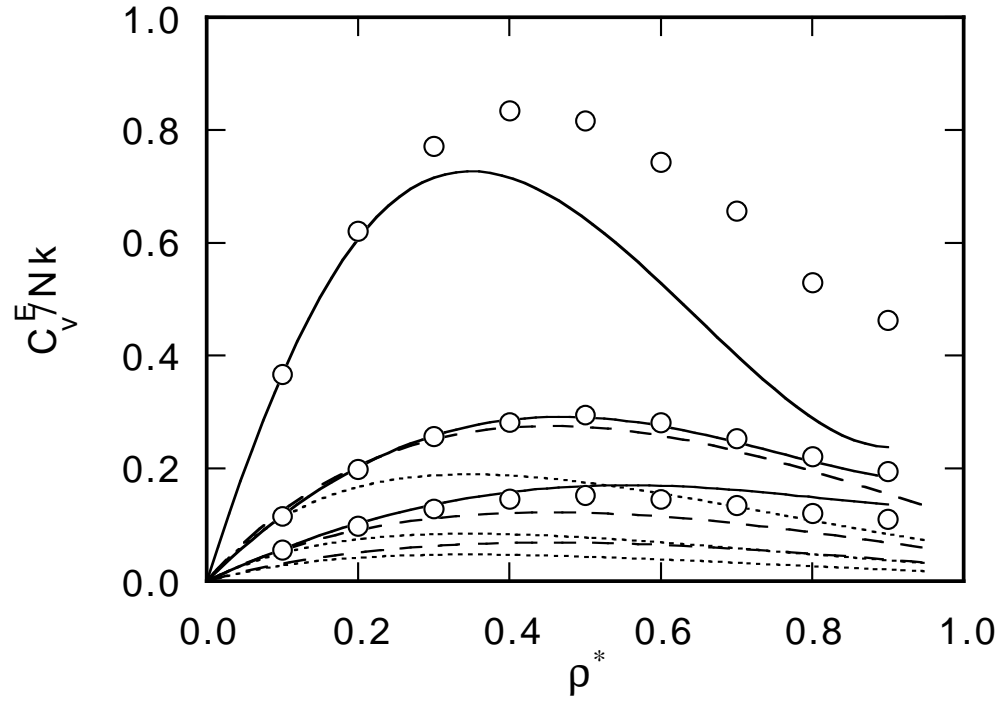


FIG. 2: As in Fig. 1 for  $\lambda = 1.2$ , except that the temperatures are  $T^* = 1.0$ ,  $T^* = 1.5$ , and  $T^* = 2.0$ , respectively, from top to down.

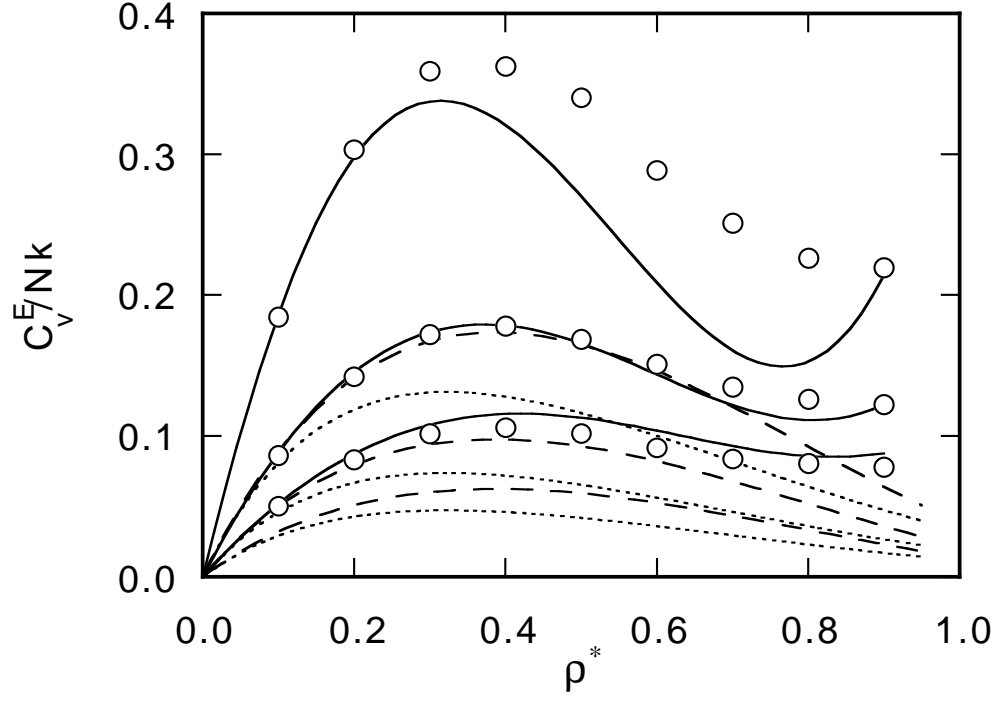


FIG. 3: As in Fig. 1 for  $\lambda = 1.3$ , except that the temperatures are  $T^* = 1.50$ ,  $T^* = 2.0$ , and  $T^* = 2.5$ , respectively, from top to down.

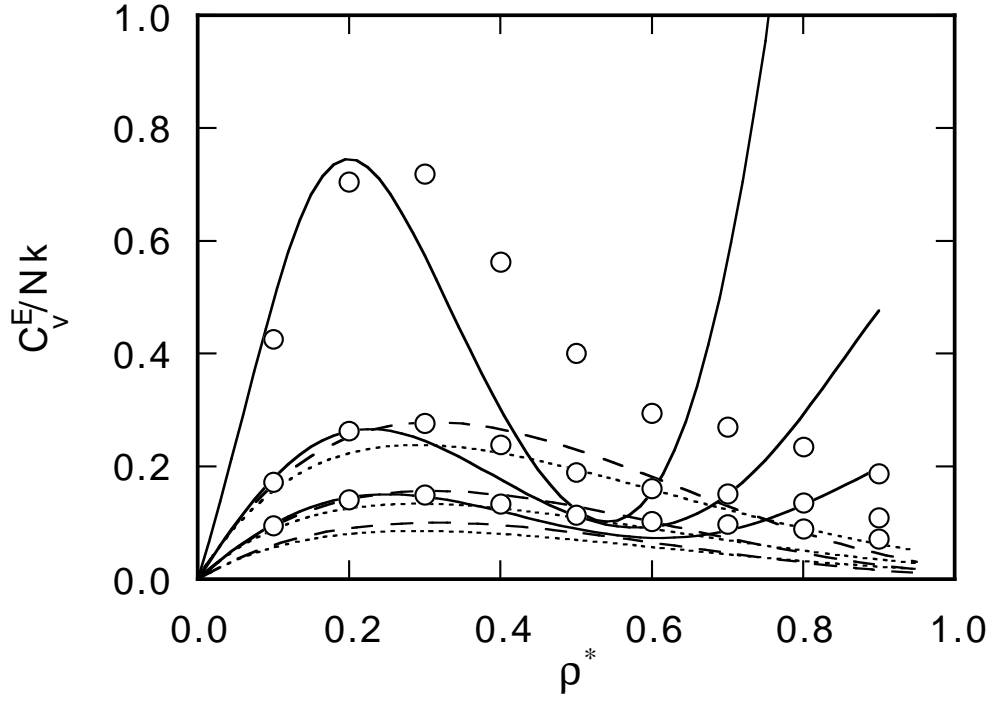


FIG. 4: As in Fig. 1 for  $\lambda = 1.5$ , except that the temperatures are  $T^* = 1.50$ ,  $T^* = 2.0$ , and  $T^* = 2.5$ , respectively, from top to down.